

PACS numbers: 79.20.Ds; 52.38. – r
DOI: 10.1070/QE2007v037n11ABEH013521

Dynamics of surface processes in a transparent dielectric exposed to laser radiation

S.V. Vasil'ev, V.I. Nedolugov

Abstract. **High-speed interference filming is used to study the dynamics of development of the change region of a surface vapour – plasma formation under the action of laser radiation with a power density up to 10^7 W cm^{-2} and a pulse duration of ~ 1 ms on polymethyl methacrylate samples of thickness up to 1 cm. Experiments show that damage region is mainly produced due to a thermal mechanism along with the possible effect of the emerging elastic vibrations. It is also shown that the damage takes place predominantly at the initial stages of the process (up to 100 μs) due to shielding of the sample by a vapour – plasma cloud and scattering of radiation from the liquid-drop phase.**

Keywords: *laser damage region, transparent dielectric, high-speed interference filming*.

1. Introduction

A large number of experimental and theoretical works [1 – 6] have been devoted to the analysis of damage of transparent solids exposed to laser radiation. This is explained by the fact that transparent solids are widely used in laser technology (active elements, laser beam shaping and transport systems, nonlinear transducers). Significant advances have been achieved by using polymethyl methacrylate (PMMA) for preparing polymer matrices for laser active elements. This is due to relative simplicity of preparation of such matrices and their high optical quality [7 – 9].

The main disadvantage of PMMA is its low radiation resistance. The damage of transparent solids can be caused by various mechanisms [4]. The realisation of a particular mechanism is determined by various external factors and the presence of absorbing inclusions in a sample. Heating of an absorbing inclusion by focused laser radiation of above-threshold intensity is accompanied by the appearance of thermoelastic stresses leading to the bulk damage of a polymer. In addition, elastic waves emerging during the formation and growth of a crater can also affect the damage nature. Therefore, it is important to find the peculiarities of the damage of transparent polymers under various conditions of laser action. Analysis of the action of ~ 1-ms laser pulses of a complex shape with power densities of 10^6 – 10^7 W cm^{-2} on PMMA samples is also important because laser radiation with these parameters causes not only the destruction of a target but also changes the atomic – molecular structure of a sample [10].

The aim of our work is to study the dynamics of destruction zone formation under various conditions of laser action on PMMA as well as the accompanying surface processes, such as the expansion of the liquid drop phase and the formation and development of a vapour – plasma cloud.

2. Experimental

Figure 1 shows the experimental setup used in the study. Radiation from free-running GOR-100M ruby laser (*1*) emitting 1.2-ms, 0.694-μm pulses is focused by lens (*2*) to sample (*3*). The diameter D of the laser spot with sharp edges was varied during experiments from 1 to 2 mm.

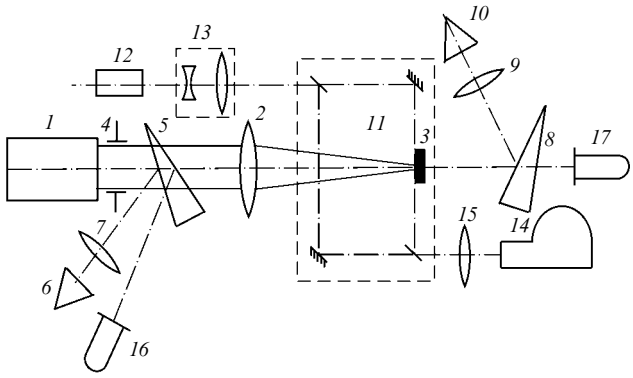

Figure 1. Scheme of the experimental setup.

The experimentally determined size of the focal (caustic) region of lens (*2*) obtained by using laser (*1*) did not exceed 2 mm. A part of the radiation (~ 4 %) was reflected from the front face of glass wedge (*5*) to IMO-2N power meter (*6*) whose entrance pupil was located in the focal plane of lens (*7*). The laser pulse energy E_0 varied from 5 to 60 J. A part of the radiation (~ 4 %) passing through sample (*3*) was directed with the help of second glass wedge (*8*) and lens (*9*) to another IMO-2N power meter (*10*). The absorption

S.V. Vasil'ev, V.I. Nedolugov Yanka Kupala Grodno State University, ul. Ozheshko, 230023 Grodno, Belarus;
e-mail: s.vasiljev@grsu.by

Received 15 January 2007; revision received 4 April 2007
Kvantovaya Elektronika **37** (11) 1047 – 1050 (2007)
Translated by Ram Wadhwa

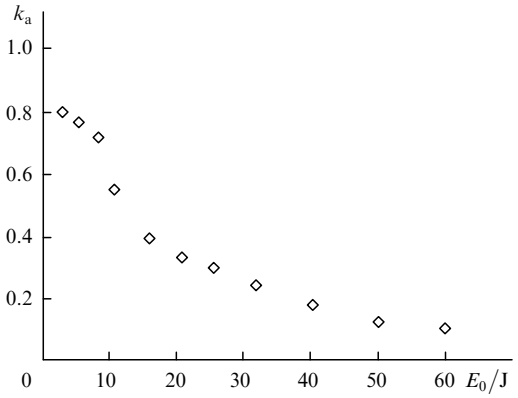

Figure 2. Dependence of the absorption coefficient k_a of laser radiation on the incident energy E_0 for a 7-mm-thick PMMA sample.

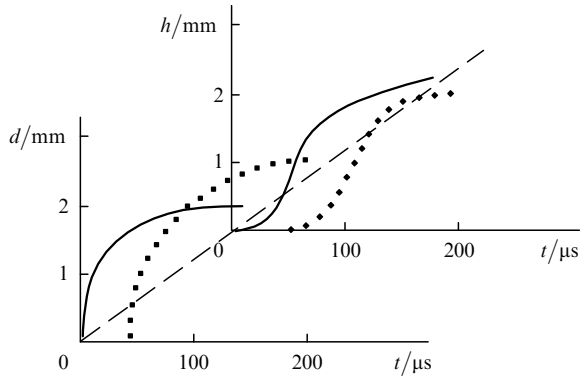

Figure 3. Time dependences of the diameter d and depth h of a crater for $E_0 = 30$ J, $D = 1$ mm and $l = 7$ mm (the solid curve corresponds to crater parameters on the rear side of the sample, and the dashed curve corresponds to parameters on the front side).

coefficient k_a was determined from the readings of power meters (*6*) and (*10*) (Fig. 2). Coaxial FEK-14 photoelectric elements, (*16*) and (*17*), the signal from which was fed to the input of the S8-13 oscillographs, were used for recording the laser pulse shape.

The surface processes occurring in sample (*3*) exposed to laser radiation were studied by placing it in one of the arms of Mach–Zehnder holographic interferometer (*11*). The interferometer was illuminated by free-running 0.694-μm ruby laser (*12*). The transverse mode selection in the probe laser was performed with an intracavity aperture, while longitudinal modes were selected with a Fabry–Perot etalon, which was used as the output mirror. The probe radiation was directed to collimator (*13*) which formed a parallel light beam whose diameter (3 cm) was larger than the thickness of the sample being irradiated. This made it possible to follow the growth of the crater, the evolution of the vapour–plasma cloud, as well as the formation and propagation of elastic waves in the sample.

The interferometer coupled with high-speed SFR-1M camera (*14*) whose film plane was conjugated with the meridional cross section of the laser beam acting on the sample with the help of objective (*15*). The high-speed camera operated in the time magnifying regime and provided a spatial field resolution of the object ~15 μm. The time resolution was ~1 μs.

3. Peculiarities of crater formation in PMMA

Exposure of a 1-mm thick sample to laser radiation led to the formation of craters on its front and rear faces because the focal (caustic) region of focusing lens (*2*) was larger than the sample thickness. The evolution dynamics of such craters in time is described in [10].

When laser radiation was focused on the front face of a sample of thickness 3 mm or more, craters were formed only on this face. The evolution dynamics of craters on the front face of the sample for the laser radiation parameters used in our experiments is described in detail in [11].

The situation was quite different when laser radiation was focused on the rear face of a 7-mm-thick sample. At the initial stage (~20 μs), the crater was first formed on the rear face and then on the front face. Figure 3 demonstrates the growth of both these craters.

The growth dynamics of craters on both sides of the sample is nearly identical. The initial growth of the crater at the rear surface is explained by the absorption of focused laser radiation on the PMMA surface. Later, within 50 μs, the front surface, the interface between the two media having a higher inhomogeneity than the bulk of the sample (which is already overheated by this time) begins to play an important role in the absorption of laser radiation. The formation of a crater at the front face and the surface vapour–plasma formation prevent the passage of laser radiation, although a part of radiation is incident on the rear side of the sample and even passes through it (Fig. 4). The crater on the rear side is slightly elongated along the laser beam because the main part of the radiation energy after its formation is absorbed by the crater surface facing the laser.

The experimental time dependences of the crater diameter d and depth h (Fig. 3) are nonlinear. The initial rapid increase in d and h slows down abruptly after about 100 μs.

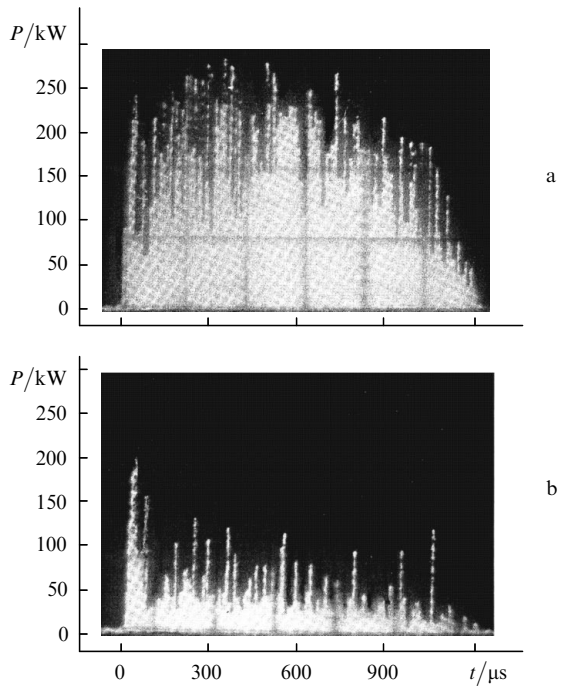

Figure 4. Oscillograms of laser pulses (a) before and (b) after passage through a 7-mm-thick PMMA sample.

Note that the crater size both at the front and rear sides of the sample increases first predominantly due to an increase in its diameter (Fig. 3), and a three-dimensional growth of the crater begins after the value $\sim 1.5D$ is achieved.

This can be explained as follows. First, the crater grows due to a uniform (and weak) absorption of laser radiation in the transparent medium. PMMA softens rapidly (the softening temperature is $\sim 120\,^{\circ}\mathrm{C}$ [12]) and vapour (subsequently, vapour–plasma) plume is formed whose size exceeds the focusing spot diameter (Fig. 5). The sample surface is heated due to transfer of heat from the vapour–plasma plume, facilitating an increase in the crater diameter.

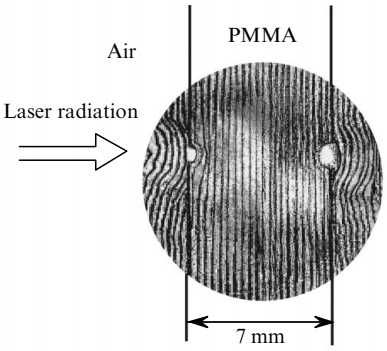

Figure 5. Interference pattern illustrating the action of laser radiation on PMMA at the instant $t = 50$ μs from the beginning of the action of laser radiation with $E_0 = 30$ J, $D = 1$ mm.

As a result, the energy absorption by the softened and less transparent PMMA at the front side of the sample along the laser beam increases. The heat flux is equalised over all directions and the evaporation becomes three-dimensional. The second stage of the process, in which $\Delta d \sim \Delta h$, sets in. At the same time, the amount of energy reaching the rear surface of the sample decreases sharply. Absorption mainly takes place at the crater surface facing the laser. As a result, the damage region is stretched along the laser radiation propagation direction.

Note that the crater growth practically terminates within $t_{\max} \sim 100$ μs (see Fig. 3) after irradiation of the sample by 1.2-ms pulses. This means that for laser power densities used in our experiments for $t > t_{\max}$, the absorbed energy was insufficient for maintaining the vaporisation temperature at the surface of the formed crater. This can be explained by an increase in heat removal from the increased surface area of the crater due to a partial shielding of laser radiation by the plasma plume (by this time, the power density q in some laser spikes achieves its maximum value of $\sim 10^7$ W cm^{-2}) and by scattering of radiation from the liquid-drop phase. Local vaporisation, which is responsible for a much smaller mass removal, still continues.

The damage of a sample produced by focusing laser radiation in the irradiated region passed to the front face of the sample, which was followed by the removal of the liquid-drop phase from the damaged region in the direction of the laser. The volume of the escaping material was double the amount of material escaped upon focusing laser radiation at the sample surface (Fig. 6). This can be explained by thermal explosion of an absorbing inclusion, resulting in the removal of a large mass under the action of the pressure produced.

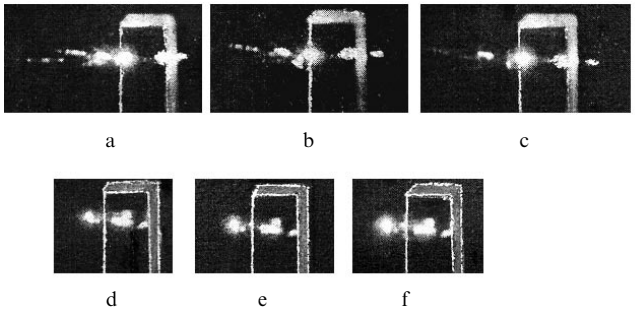

Figure 6. Shadow patterns of the action of laser radiation on a sample at the instants $t = 54$ (a, d), 62 (b, e) and 70 μs (c, f) from the beginning of the action of laser radiation focused on the rear side (a–c) and into the bulk (d–f) of the PMMA sample with $E_0 = 30$ J, $D = 1$ mm, and $l = 7$ mm.

Figure 7 shows a photograph of the sample after exposure to laser radiation. One can see that upon focusing radiation at the rear side, the sample is damaged in the form of cracks in various directions. This can be explained as follows. The optical breakdown of transparent polymers is related to the absorbing inclusions which are always present in the sample. In addition, elastic waves are produced in the sample during the crater growth [13, 14]. Figure 8 shows the interference pattern demonstrating spherical waves propagating in the sample, which were recorded by high-speed filming. The wavefront propagation velocity calculated from the interferograms is ~ 2.7 km h^{-1}.

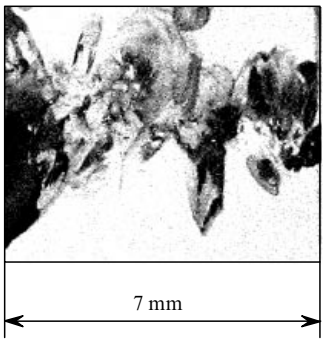

Figure 7. Photograph of a PMMA sample after exposing to laser radiation with $E_0 = 30$ J, $D = 1$ mm.

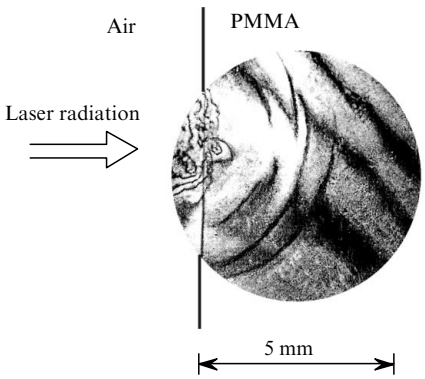

Figure 8. Interference pattern of an acoustic wave in PMMA at the instant $t = 50$ μs from the beginning of the action of laser radiation with $E_0 = 30$ J, $D = 1$ mm.

The pressure of elastic vibrations produced in the material being processed was detected with a TsTS-19 piezoceramic sensor equipped with a device for compensating reflections.

The maximum pressure of elastic vibrations calculated from the oscillograms was ~ 5 kPa.

Cracks appear in the sample within 80 – 100 μs after the beginning of laser action. In our opinion, this may explained as follows. At the stage of stabilisation of the growth of geometrical parameters of the crater (when it achieves its maximum size), the highest thermoelastic stresses are produced which may lead to the formation of cracks. In addition, due to the low thermal conductivity and low absorption coefficient of PMMA, its volume is heated only after 80 – 100 ms. Because the absorption coefficient of inclusions may depend strongly on temperature, thermal instability may arise in the absorption region [6], resulting in the damage of the sample. In addition, elastic vibrations produce stresses in the sample [15], which can also cause the sample damage.

4. Escape of the liquid-drop phase and shielding of the target surface

The escape of the liquid-drop phase begins within 10 μs after the beginning of laser action. The maximum size of drops at the initial stage of their formation (at the moment of their detachment from the sample) is approximately equal to the size of the laser focus spot. The drops are then split in the field of the laser beam. The initial escape rate determined from the shadow patterns (Fig. 6) is ~ 100 m s^{-1}. The escape of drops with a certain periodicity was observed during the entire exposure time. The periodicity of escape may be explained as follows. Laser radiation heats the PMMA surface and causes evaporation of a part of the sample, and heats it until the formation of a plasma. [The plasma formation is observed in the interference patterns (Figs 5 and 8).] The surface plasma strongly absorbs laser radiation and laser radiation is also defocused in the plasma. As a result, the radiation intensity at the sample surface decreases and the supply of the sample material to the plasma terminates. The vapour – plasma formation is destroyed, the sample shielding decreases, and the process is repeated again.

Figure 4 shows the oscillograms of the laser pulse before and after passage through the PMMA sample, which were obtained with photocells (*16*) and (*17*). Note that the laser radiation intensity decreased sharply after passing through the sample (after about 50 μs). This is explained by its shielding the vapour – plasma plume (by this time, the power density in some laser spikes achieves $\sim 10^7$ W cm^{-2}) which is probably formed in the escaping liquid-drop phase. A part of radiation passing through the sample and obtained as the difference in the readings of power meters (*6*) and (*10*) was virtually independent of the sample thickness and varied from 80 % (for an energy of 1 J) to 10 % (50 J) for a focus spot area of ~ 1 mm^2 (Fig. 2). The sharp decrease occurs for a laser radiation energy of ~ 10 J (corresponding to the pulse-averaged power density of laser radiation equal to $\sim 10^6$ W cm^{-2}), indicating the beginning of plasma formation and hence shielding of the sample.

5. Conclusions

It has been shown that the efficient growth of a crater produced by a ~ 1-ms laser pulse at the surface of a transparent dielectric continues for no more than 100 μs. At first, the area of the crater increases and, after its size becomes more than double the size of radiation focal spot, the three-dimensional growth of the damage region begins. The crater growth dynamics is determined during first 100 μs (mainly by evaporation mechanism). After this, the growth of the crater substantially slows down due to shielding of the sample by the plasma plume, scattering of radiation from the liquid-drop phase, and impossibility to implement the hydrodynamic mechanism in organic compounds of the PMMA type.

We have shown experimentally that the laser damage region is produced due to thermal heating of absorbing inclusions in the sample and, possibly, due to the effect of elastic vibrations.

References

1. Ashkinadze B.M., Vladimirov V.I., Likhachev V.A., Ryvkin S.M. *Zh. Eksp. Teor. Phys.*, **50**, 1187 (1966).
2. Manenkov A.A., Nechtailo V.S. *Kvantovaya Elektron.*, **7**, 616 (1980) [*Sov. J. Quantum Electron.*, **10**, 347 (1980)].
3. Manenkov A.A., Matyushin G.A., Nechitailo V.S. *Kvantovaya Elektron.*, **11**, 839 (1984) [*Sov. J. Quantum Electron.*, **14**, 568 (1984)].
4. Manenkov A.A., Prokhorov A.M. *Usp. Fiz. Nauk*, **148**, 179 (1986).
5. Dyumaev K.M., Manenkov A.A., Maslyukov A.P., et al. *Trudy IOFAN*, **33**, 3 (1991).
6. Koldunov M.F., Manenkov A.A., Pokotilo I.L. *Kvantovaya Elektron.*, **32**, 623 (2002) [*Quantum Electron.*, **32**, 623 (2002)].
7. Gromov D.A., Dyumaev K.M., Manenkov A.A., et al. *Izv. Akad. Nauk SSSR, Ser. Fizich.*, **46**, 1956 (1982).
8. Dyumaev K.M., Manenkov A.A., Maslyukov A.P., et al. *Kvantovaya Elektron.*, **10**, 810 (1983) [*Sov. J. Quantum Electron.*, **13**, 503 (1983)].
9. Bezrodnyi V.I., Derevyanko N.A., Ishchenko A.A., Karabanova L.V. *Zh. Tekh. Fiz.*, **71**, 72 (2001).
10. Vasil'ev S.V., Voina V.V., Ivanov A.Yu., Liopo V.A. *Kvantovaya Elektron.*, **25**, 1023 (1998) [*Quantum Electron.*, **28**, 997 (1998)].
11. Vasil'ev S.V., Ivanov A.Yu., Nedolugov V.I. *Kvantovaya Elektron.*, **21**, 324 (1994) [*Quantum Electron.*, **24**, 302 (1994)].
12. Babichev A.P., Babushkina A.N., Bratkovskii A.M., et al. *Fizicheskie velichiny, Spravochnik* (Handbook of Physical Quantities) (Moscow: Energoatomizdat, 1991).
13. Ashmarin I.I., Bykovskii Yu.A., Gridin V.A., et al. *Kvantovaya Elektron.*, **6**, 1730 (1979) [*Sov. J. Quantum Electron.*, **9**, 1019 (1979).
14. Lyamshev L.M. *Usp. Fiz. Nauk*, **135**, 637 (1981).
15. Ashmarin I.I., Bykovskii Yu.A., Larkin A.I., et al. *Zh. Tekh. Fiz.*, **43**, 2397 (1973).